Production of neutral fragments from the dissociation of fast H_3^+ ions

Ginette Jalbert and L. F. S. Coelho

Instituto de Física, Universidade Federal do Rio de Janeiro, Caixa Postal 68528,
Rio de Janeiro, 21945, RJ, Brazil

N. V. de Castro Faria

Departamento de Física, Pontifícia Universidade Católica do Rio de Janeiro,
Caixa Postal 38071, Rio de Janeiro, 22453, RJ, Brazil

H_3^+ ions of velocity 4–7 a.u. have been passed through targets of several noble gases, He, Ne, Ar, and Xe, and the production of single H atoms, single H_2 molecules, and pairs of H atoms has been studied. These are the main dissociation channels leading to the production of atomic and molecular neutral particles, other processes—formation of one H_3 molecule, three H atoms, or one H_2-H pair—being negligible as they require electron capture by these fast projectiles. The yields for the processes under study were measured as a function of target pressure, and the production cross sections extracted from the low-pressure region of the yield curves.

I. INTRODUCTION

During the past decade the H_3^+ ion has received considerable attention due, first of all, to its relevance as the simplest polyatomic molecule. This intrinsic importance, together with the increasing availability of computing power, led to a rising number of molecular-structure calculations [1]. It is also important for covalent-cluster studies, nucleating H_2 molecules in order to form H_n^+ clusters [2]. Even more important is the interest of this ion for basic and applied atomic-collision physics, on topics ranging from astrophysics to plasmas. For instance, recent theoretical models [3] point to H_3^+ as the intermediate needed to form complex molecules in the interstellar space, through reactions like $X + H_3^+ \rightarrow XH^+ + H_2$. Also, as the maximum yields for neutral atomic hydrogen coming from H_3^+ high-energy destruction are larger than the ones obtained from lighter projectiles, H^+ and H_2^+, intense beams of fast neutral particles may be produced. Consequently, these H_3^+ beams allow atomic collision experiments to be performed below the low-energy limit that exists for atomic beams coming directly from the ion source (this threshold is a characteristic of each accelerating system), and also may be useful for fusion plasma studies [4].
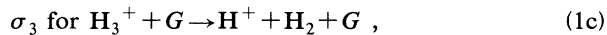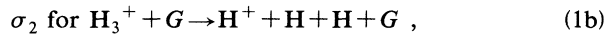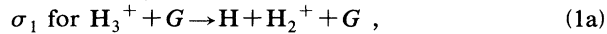
Concerning atomic collisions, the H_3^+ collisional dissociation has been studied mostly at low energies and for some specific channels, such as the ones leading to H^-, H_2^+, or $H + H_2$ production [5–10], although there are studies at intermediate and high energies [11–17]. It must be pointed out, however, that, even with the above-mentioned work and the references therein, there are few destruction cross-section measurements, either total or for any specific channel (see, for example, the review made by Tawara *et al.* [18] of electron impact H_3^+ destruction).

The main drive for the low-energy collision work has been the study of the potential-energy surfaces and the geometry of excited molecular states. Most of the works listed in Refs. [5–7] achieved this by measuring the H^- energy and angular distributions in the kilo-electron-volt energy range, although some give distributions for other fragments such as H^+ and H_2^+. The dissociative recombination of H_3^+ ions, in particular when it leads to the simultaneous H and H_2 production, has been investigated by several groups, with cross sections being obtained of energies of 1 eV and lower [8] and around a few kiloelectron volts [9]. Cross sections for the simultaneous production of two hydrogen atoms were also measured for energies of tens of electron volts [10], as a test for the excited state content of H_3^+ beams coming from ion sources in different operating conditions.
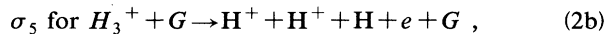
Intermediate- and high-energy H_3^+ collisions have received, since the pioneering works [11], less attention [12–17]. There are few studies for noble-gas targets, with H_2 receiving most of the attention, and the projectile energies rarely exceed 1 MeV. Of particular interest for the work related here are the few measurements of cross sections for producing neutral particles. Berkner *et al.* [11] reported measurements of cross sections for several fragmentation channels, with projectile energies ranging from 0.4 to 1.8 MeV (velocities going from 2.3 to 4.9 a.u.) and the targets being H_2, N_2, and Li. The fragments were measured in coincidence and a low-transmission mesh was employed in order to discriminate between the arrival at the detector of two H atoms or one H_2 molecule. The probabilities of the several fragmentation channels for 0.4–0.8-MeV H_3^+ ions ($v = 2.3$ a.u. to 3.3 a.u.) colliding with H_2, Ar, and air targets were measured by Nir *et al.* [12]. Afterwards the same group presented measurements [12] at lower velocities (1.4–2.0 a.u.) for the D_3^+ colliding with H_2 and Ar. Both works employed

coincidence experimental setups and in the latter a mesh was used to discriminate "D_2" and "$2D$" events and, as the corresponding destruction cross sections were not available, these measured probabilities could not lead to cross-section values. Capture cross sections in Ar [13] and the growth curve for H^- production in Ne [14] were measured, although not systematically, together with H_3^+ destruction cross sections.

Finally, several fast H_3^+ collision processes were recently measured in our laboratory [15–17], the first of them being the H_3^+ destruction in noble gases [15]. The knowledge of the destruction cross section is important for the present work as it allows a better modeling of the neutral yields as function of the target pressure and also the monitoring of the beam intensity. The destruction is unlikely to proceed by electron capture [13], although this may be so at low energies [19], and goes through mainly by the following dissociative excitation,

$$\sigma_1 \text{ for } H_3^+ + G \rightarrow H + H_2^+ + G \ , \tag{1a}$$

$$\sigma_2 \text{ for } H_3^+ + G \rightarrow H^+ + H + H + G \ , \tag{1b}$$

$$\sigma_3 \text{ for } H_3^+ + G \rightarrow H^+ + H_2 + G \ , \tag{1c}$$

and ionization channels (single-electron loss),

$$\sigma_4 \text{ for } H_3^+ + G \rightarrow H_2^+ + H^+ + e + G \ , \tag{2a}$$

$$\sigma_5 \text{ for } H_3^+ + G \rightarrow H^+ + H^+ + H + e + G \ , \tag{2b}$$

where σ_i is the cross section of each reaction.

The cross sections measured in the present work are the ones for producing a single H, two hydrogen atoms, and a neutral hydrogen molecule. They are written respectively as σ_0, σ_{00}, and σ_M, where σ_0 is equal to the $\sigma_1 + \sigma_5$ sum [processes (1a) and (2b)], σ_{00} to σ_2 [process (1b)] and, finally, σ_M to σ_3 [process (1c)]. Four noble gases were employed as targets, He, Ne, Ar, and Xe, and the projectile velocities went from 4 to 7 a.u. The cross sections for single (σ_0) and double mass events $(\sigma_{II} = \sigma_{00} + \sigma_M)$ were directly measured for these targets. In order to discriminate H_2 from $2H$ events, for the Ar case data were taken with and without a mesh in front of the detector of neutral molecules.

II. EXPERIMENTAL ARRANGEMENT

The incident H_3^+ beam was obtained from a standard radio-frequency ion source and accelerated by the PUC/RJ 4-MV Van de Graaff (HVEC) accelerator, with energies in the 1.2–3.7 MeV range. The beam is mass energy analyzed by a 90° magnet and collimated to a di-

ameter of less than 0.3 mm by four micrometric sliding slits. This very strong collimation reduced the beam intensity to values that were always maintained smaller than 10^3 particles per second allowing the use of surface barrier detectors to detect the neutral molecules and the transmitted H_3^+ ions. A scheme of the experimental setup is shown in Fig. 1. Due to these high kinetic energies, the cross sections for the different channels are not expected to be dependent on the possible excited rovibrational-level distribution [8,10,20], as confirmed by recent measurements of the H_3^+ destruction [15].

The gas-target cell, 10 cm long, is coupled to a two-axis goniometer for easy alignment. It has an entrance and an exit apertures of 0.5 and 2.0 mm, respectively, and is placed in a chamber evacuated by a 200-l/s diffusion pump. Vacuum impedances isolate this chamber from the remaining beam line, where the vacuum is maintained by two diffusion pumps, each one installed nearby one impedance. With this arrangement a pressure gradient of a factor of 10^3 was obtained between the gas cell and the surrounding vacuum. Even for a target-detector distance 15 times larger than the cell length this residual pressure had only a small influence on the neutral products, acting as an additional target with a thickness that is about 1% of the one for the gas cell. This residual atmosphere is composed mainly of impurities, including air and water desorbed by the pipe which brought the gas to the cell, residual gases from the background, and gases from previous experimental runs. Several precautions were taken to avoid this problem including the use of a cooling system in which the He and Ne gases leaving the bottles traverse a liquid-nitrogen trap before entering the cell. The gas-target pressure was measured employing a thermocouple device, calibrated against a McLeod gauge as described in Ref. [21]. The uncertainty arising from the thermocouple calibration was estimated to be less than 10%, being due to both the calibration procedure and to the McLeod-gauge uncertainty. The nominal purities of target gases were 99.99%.

The gas cell is followed by another magnet with seven exits, one in the beam line direction and three on each side at the angles $\pm 15°$, $\pm 30°$, and $\pm 45°$. The several neutral events—the arrival of single H, single H_2, and two simultaneous H particles—were detected at zero degrees by a large (25 mm diameter) surface-barrier detector and this, together with the H_3^+ detection at $+15°$, allows the yields to be obtained. The output of the detectors also allows the beam energy and composition to be continuously monitored with oscilloscopes. The molecular-explosion cone section in the worst case occupies a small fraction of the detector surface. Another detector, with a diameter
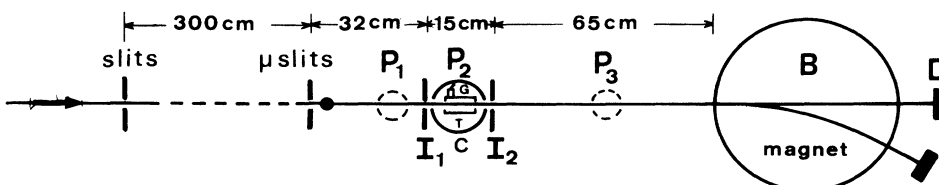

FIG. 1. Experimental setup: T is the gas cell, G the vacuum gauge, I_i vacua impedances, P_i diffusion pumps, and D surface barrier detectors (the drawing is not entirely to scale).

~15 mm, was employed for the H_3^+ ions and, in order to center both beams simultaneously, this detector could be moved in a plane normal to the detected beam. To avoid pileup problems the counting rate of the H_3^+ detector was less than 10^3 counts per second, as already stated. The double-height pulses obtained when H_2 or two simultaneous H atoms entered the detector were clearly resolved from single pulses of isolated H atoms, resulting in two peaks each counted in a different scalar. A third scalar is used to monitor the H_3^+ pulses. Starting and stopping the counting was made by opening and closing a beam stopper.

In the argon case, a mesh was employed to discriminate between an H_2 molecule and two H atoms. The mesh transmission t has a value of 38%, directly obtained from transmission experiments of proton and alpha-particle beams, which is comparable with the value extracted from the neutral measurements, as will be shown in the next section. The holes of the mesh are approximately squares that are $120 \times 120 \ \mu m^3$. Spectra were taken with and without the mesh. Briefly, when two H atoms are produced, they arrive simultaneously at the detector site. The atom-atom distance is of the order of millimeter, owing to the sharing of the excess internal energy during the dissociation. Each hydrogen atom could, independently, traverse the grid or be stopped there, resulting in three possibilities. When both cross the grid an energy of $2E/3$ is deposited in the detector and, if only one is transmitted, the deposited energy is $E/3$, where E is the projectile energy. Otherwise, when only an H atom or an H_2 molecule is produced in the collision it either crosses the grid or it does not. In case it does, it will deposit an energy $E/3$ if it was an atom and $2E/3$ if it was a molecule. Consequently, algebraic equations depending on t and t^2 may be written relating these three events (single H, single H_2, or double H production) to the $E/3$ and $2E/3$ peaks in spectra taken with and without the mesh. In particular, the $H+H$ and H_2 cross sections can then be separately obtained. This analysis procedure will be fully described in the next section.

Statistical errors were ±5% in the most unfavorable cases. Including also estimations of the error due to the vacuum quality and to the fitting procedure, an average uncertainty of at the maximum ±12% must be assigned to the absolute cross sections measured in this work, except for the situation where the mesh technique was employed. In that case the maximum propagated errors could be 20% for producing two H atoms and 50% for a single H_2 molecule, as will be discussed in the next section.

III. DATA ANALYSIS AND RESULTS

Multiple-collision processes depend upon the initial and the final states of the particles involved in the intermediate collisions and a full understanding requires the knowledge of a rather large number of cross sections. For example, if one is measuring the direct production of a pair of H atoms–$H_3^+ \rightarrow H+H+H^+$–the final states may not be relevant but this is not so in two-step processes such as $H_3^+ \rightarrow H_2(v)+H^+ \rightarrow H+H+H^+$ or

$H_3^+ \rightarrow H_2^+(v)+H \rightarrow H+H^++H$. As further examples of these higher-order processes one has (1) the H production followed by its destruction, (2) the production of two H atoms followed by one or both suffering an electron-loss collision, and (3) the H_2 production and its breakup leading to one or two H atoms. Although the analytical descriptions of the H_3^+ attenuation and the H_2 production are easily done, as will be shown, the multiple-collision production of one or two H atoms may only be described by very simplified models which, among other assumptions, neglect electron-capture and double-electron-loss processes.

It is straightforward to show that, upon neglecting electron capture by H_2^+ and H_3^+ ions, one has

$$N_{H_3^+} = N_i e^{-\sigma_d^{H_3^+} \pi}, \tag{3a}$$

$$N_M = N_i \sigma_M \left[\frac{e^{-\sigma_d^{H_3^+} \pi} - e^{-\sigma_d^{H_2} \pi}}{\sigma_d^{H_2} - \sigma_d^{H_3^+}} \right], \tag{3b}$$

where $N_{H_3^+}$ and N_M are, respectively, the measured flows of H_3^+ and H_2 molecules, N_i is the flow of H_3^+ ions inciding upon the target, $\sigma_d^{H_3^+}$ and $\sigma_d^{H_2}$ are the destruction cross sections and π, the target thickness, is the product of the target length l by its density n.

The situation becomes much more complex when one considers the production of one or two neutral hydrogen atoms, as they may arise from a variety of processes. Again we will neglect electron-capture channels. Additionally, the negative-ion production and the double-electron loss will also be neglected. Even so ten cross-section values will be needed: σ_1 to σ_5 for the processes in Eqs. (1) and (2), $\sigma_d^{H_3^+}$ for the H_3^+ destruction, σ_{01} for electron loss in a H projectile, and

$$\sigma_6 \text{ for } H_2^+ + G \rightarrow H + H^+ + G, \tag{4a}$$

$$\sigma_7 \text{ for } H_2 + G \rightarrow H + H + G, \tag{4b}$$

$$\sigma_8 \text{ for } H_2 + G \rightarrow H + H^+ + e + G. \tag{4c}$$

Considering the processes in a second-order approximation, and this means considering only two collisions for each projectile, it is straightforward to obtain

$$N_0 = N_i \pi [\sigma_0 (1 - \tfrac{1}{2}(\sigma_{01} + \sigma_d^{H_3^+})\pi)$$
$$+ (\sigma_4 \sigma_6 + \sigma_2 \sigma_{01} + \sigma_3 \sigma_8)\pi], \tag{5a}$$

$$N_{00} = N_i \pi [\sigma_{00}(1 - \tfrac{1}{2}(2\sigma_{01} + \sigma_d^{H_3^+})\pi) + (\sigma_1 \sigma_6 + \sigma_3 \sigma_7)\pi], \tag{5b}$$

where N_0 is the number of events with only one neutral atom being produced and N_{00} is the number for two atoms. It is obviously not possible to extract with reasonable precision ten cross sections from the fit of two growth curves to expressions (5a) and (5b), mainly when it is noted that these expressions themselves are also

rough approximations.

In the single-collision process limit only three cross sections are apparently needed in order to describe N_0, N_M, and N_{00}, as one can get from Eqs. (3b), (5a), and (5b) in the low-pressure limit:

$$N_M = N_i \sigma_M \pi , \tag{6a}$$

$$N_0 = N_i \sigma_0 \pi , \tag{6b}$$

$$N_{00} = N_i \sigma_{00} \pi . \tag{6c}$$

However, in order to account for the incident beam attenuation in a nonzero-thickness target at least an additional fourth cross section is needed and, as indicated by expression (3a), the measured H_3^+ flow must be multiplied by $e^{\sigma_d^{H_3^+} \pi}$ to get the incident N_i flow.

A. Analysis of the data taken without the grid

From the data taken without the grid, we have obtained the cross section for production of hydrogen atoms σ_0 and σ_{II}, the total production of neutral particles with two thirds of the H_3^+ initial energy, i.e., the sum of σ_{00} and σ_M. However, as previously discussed, the complexity of the phenomena does not allow fitting the measured numbers N_0 and N_{II} ($N_{00} + N_M$) with basic expressions. We have then proceeded as follows: the experimental results N_0 and N_{II} were first normalized to the number of incident particles N_i and a least-square fit to a polynomial power series of π ($B + \sigma\pi + \alpha\pi^2 + \beta\pi^3 + \cdots$), was then performed. B corresponds to the numbers of particles at zero pressure, α and β account for multiple processes, and σ is the desired cross-section production. When the data corresponding to high-pressure values were considered, polynomials of third or even fourth order were needed to fit the data. However, a lower order, say two, was sufficient to obtain a good fit when only the low-pressure measured values were used. In any case, the cross sections obtained agree with the others. We have considered the inverse of the standard deviation associated with statistical uncertainties, set equal to the square root of the measured values, as the weight of the data.

We present in Tables I and II the cross sections σ_0 and σ_{II} as a function of the projectile velocity and for each gas target.

TABLE I. H production cross section σ_0 (10^{-17} cm^2).

Element	Velocity (a.u.)			
	4	5	6	7
He	3.77	3.20	2.39	1.88
Ne	15.3	13.8	11.1	9.93
Ar	31.3	27.8	22.7	21.1
Xe	31.9	34.4	27.8	27.8

TABLE II. H+H and H$_2$ production cross section σ_{II} (10^{-17} cm^2).

Element	Velocity (a.u.)			
	4	5	6	7
He	1.37	1.27	1.08	0.90
Ne	4.36	4.39	2.96	3.08
Ar	12.3	9.00	8.44	8.42
Xe	12.3	13.4	10.8	9.73

B. Analysis of the Ar data taken with and without the grid

We define N_1 and N_2 as the numbers of events respectively corresponding to one-third and two-thirds of the H_3^+ initial energy, measured when the grid is present. As before, N_0 and $N_{II} = N_M + N_{00}$ are neutral events measured without the grid.

When the size of the grid opening is much smaller than the spatial distribution of the dissociation products we have

$$N_1(\pi) = t N_0(\pi) + 2t(1-t) N_{00}(\pi) , \tag{7a}$$

$$N_2(\pi) = t N_M(\pi) + t^2 N_{00}(\pi) . \tag{7b}$$

This condition arises from the need of a negligible probability of two particles coming from different events and accidentally going through the same opening (given by the ratio of the opening area to the beam cross section). When a molecular ion dissociates, its internal energy, typically a few electron volts, is shared among the dissociation products which will move away from each other and from the dissociation center with typical velocities of $\sim 10^{-2}$ a.u. The longitudinal velocity of the primary ions is, in the least favorable case, 7 a.u. leading to values around 1 mrad for the angular spread of the beam envelope. In our experiment, the detector is situated at a distance of 1.5 m from the interaction region and, consequently, the cross-sectional radius of the explosion cone at the detector site is about 2 mm. As the grid used in our experiment has a measured opening of 120 μm, the accidental coincidence probability is one part in 1000 and Eqs. (7a) and (7b) hold true.

Normalizing the measured N_1, N_2, and N_{II} to the incident N_i values and considering that the ratios $n_0 = N_0/N_i$, $n_{00} = N_{00}/N_i$, and $n_M = N_M/N_i$ are not changed by the presence of the grid, one obtains expressions for n_M and n_{00} which may be fitted by polynomials leading to σ_M and σ_{00}. Equations (7a) and (7b) give then

$$\sigma_{00} = \frac{\sigma_1 - t\sigma_0}{2t(1-t)} , \tag{8a}$$

$$\sigma_M = \frac{\sigma_2 - t^2 \sigma_{00}}{t} . \tag{8b}$$

If one uses instead Eq. (7b) and the $N_{II} = N_M + N_{00}$ condition, the expressions for σ_M and σ_{00} become

TABLE III. H+H (σ_{00}) and H_2 (σ_M) production cross sections in Ar (10^{-17} cm^2).

Cross section	Velocity (a.u.)			
	4	5	6	7
σ_{00}	8.6	7.4	6.3	5.4
σ_M	2.0	2.1	2.3	2.4

$$\sigma_{00} = \frac{t\sigma_{II} - \sigma_2}{t(1-t)} \; , \tag{9a}$$

$$\sigma_M = \frac{\sigma_2 - t^2\sigma_{II}}{t(1-t)} \; . \tag{9b}$$

In order to minimize the propagation of fluctuations we did not employ directly the experimental cross sections σ_1, σ_2, σ_0, and σ_{II}, which appear in the right side of Eqs. (8) and (9), using instead the value coming from the fit of straight lines $1/\sigma = a + bv^2$ to the data. In the σ_0 case this procedure is based on theoretical grounds, as will be discussed in the next section.

We have performed consistency tests between the sets of equations (8) and (9), remembering that the former is independent of σ_{II} and that t has a fixed value on both sets. Concerning the first point we have verified that the sum of the σ_{00} and the σ_M cross sections, with values determined from Eqs. (8), agrees well with measurements of σ_{II} made without the grid. In the least favorable situation, $v=4$, a.u., the difference is less than 11%, within the experimental error. Now, considering t as an adjustable parameter, it is straightforward to show that

$$t = \frac{\sigma_1 + 2\sigma_2}{\sigma_0 + 2\sigma_{II}} \; .$$

Values of t determined in this less precise way for all velocities were found to be compatible with that determined by direct measurement.

Finally, we note that the cross sections calculated from the first set of equations presented uncertainties larger than the ones for the second set. For σ_{00}, in the $v=4$ a.u. case, they came down from 50% to 20%. This led us to employ Eqs. (9), with the values so obtained being presented in Table III. As already stated in the Introduction, only branching ratios for $v \sim 3$ a.u. H_3^+ ions and $v \sim 2$ a.u. D_3^+ ions are available in the literature [12]. σ_0/σ_{00} ratios may be extracted from their data and, ex-

TABLE V. Ratio $\sigma_0/\sigma_d^{H_3^+}$ for H production.

Element	Velocity (a.u.)			
	4	5	6	7
He	0.56	0.65	0.65	0.65
Ne	0.69	0.78	0.79	0.86
Ar	0.71	0.78	0.80	0.91
Xe	0.52	0.64	0.60	0.69

trapolating for our energy range, a value of 4 is obtained, agreeing very well with the data presented in Tables I and III.

IV. DISCUSSION AND CONCLUSIONS

In a recent publication [17], initially motivated by the practical interest of generating H^- beams in positive-voltage accelerators, we reported their production by fast H_3^+ ions. We have then observed that the ratio of H^- production with respect to all H_3^+ destruction channels assumed no evident dependence with respect to the targets and velocities being studied. This was not so surprising with respect to the velocity, as it presented a narrow range (4–7 a.u.), but concerning the chosen targets, going from helium $(Z=2)$ to xenon $(Z=54)$, this was not expected. Another interesting regularity observed was the reasonable fit of the H^- production cross sections by a semiempirical free-collision-type description, valid for the targets and velocities. A natural extension of that analysis would be the investigation of these properties in the case of neutral channels which present much larger probabilities than the negative one.

Taking into account the last comments and in the absence of specific calculations for these processes, the analysis of the results on the grounds of a simplified model, such as the one presented by Salpeter for H_2^+ [22], may be instructive. In the Salpeter approach the molecular-ion excitation to a self-dissociating state is considered similar to atomic ionization. The energy difference from the lowest vibrational level of their ground state, at the equilibrium internuclear distance, to the lowest self-dissociating state is defined as the equivalent of the ionization potential for a molecule and is denoted by ε. The projectile electrons are assumed to be moving freely and with the same velocity as that of the

TABLE IV. Radius parameter R, Thomas-Fermi radius R_{TF}, and R/R_{TF} ratio (all values in atomic units). R is the fitting parameter [23] as determined from the present H production data.

Element	R	R_{TF}	R/R_{TF}
He	0.134	0.703	0.190
Ne	0.077	0.411	0.187
Ar	0.070	0.338	0.207
Xe	0.042	0.234	0.180

TABLE VI. Ratio $\sigma_{II}/\sigma_d^{H_3^+}$ for H+H and H_2 production.

Element	Velocity (a.u.)			
	4	5	6	7
He	0.20	0.26	0.29	0.31
Ne	0.20	0.25	0.21	0.27
Ar	0.28	0.25	0.29	0.36
Xe	0.20	0.25	0.23	0.24

TABLE VII. Ratios $\sigma_{00}/\sigma_d^{H_3^+}$ and $\sigma_M/\sigma_d^{H_3^+}$ for H+H and H$_2$ production in Ar.

Ratio	Velocity (a.u.)			
	4	5	6	7
$\sigma_{00}/\sigma_d^{H_3^+}$	0.20	0.21	0.22	0.23
$\sigma_M/\sigma_d^{H_3^+}$	0.04	0.06	0.08	0.10

projectile, provided that this velocity is much larger than the orbital velocities of these electrons. The total cross section for a given process such as molecular ionization is then obtained by integrating the momentum-transfer differential cross section for a free electron above the threshold $q_{min} = (2m\varepsilon)^{1/2}$.

This approach, in the atomic case, is the so-called free-collision model. A large number of works was done using this model for atoms [23–25]. Reference [23], in particular, presents a simplified version of this model, adaptable to the molecular case. There, a Thomas-Fermi-like expression for the target form factors was employed, in order to avoid complex calculations for each target and each momentum transfer. With this approach, including the definition of two parameters, R and Q, empirically found to have a power-law dependence on Z, and some further simplifications [15] we could express the cross sections as simple functions of the target atomic number and of the projectile velocity, i.e, $1/\sigma = a + bv^2$. These two target-dependent parameters a and b are related to R and Q [in particular, $R = (b/a)^{1/2}/2$]. Although crude, for H$_3^+$ projectiles this model fitted well the destruction [15] and the H$^-$ production cross sections [17] and led to linear relationships between this parameter R and the Thomas-Fermi radius.

Figure 2 shows the behavior of our H data in this context. We have plotted the inverse of the cross sections as a function of the square of the projectile velocities. The data may be well described by straight lines, as the figure shows.

Numerical values for the parameter R are presented in Table IV, together with the Thomas-Fermi radii R_{TF} and the ratio R/R_{TF}. The average ratio is 0.19 ± 0.01, this uncertainty being compatible with the standard deviation of our cross sections. Remembering that the Z-dependent scaling radius R was defined [23] to obtain a universal function of r/R for the electronic density of the target, it is very encouraging to know that R is proportional to the Thomas-Fermi radius. It is also striking to notice the similar values of R extracted from this experiment and R^* coming from a previous one in H$_3^+$ destruction [16], this one leading to $R^* = 0.19R_{TF} + 0.03$.
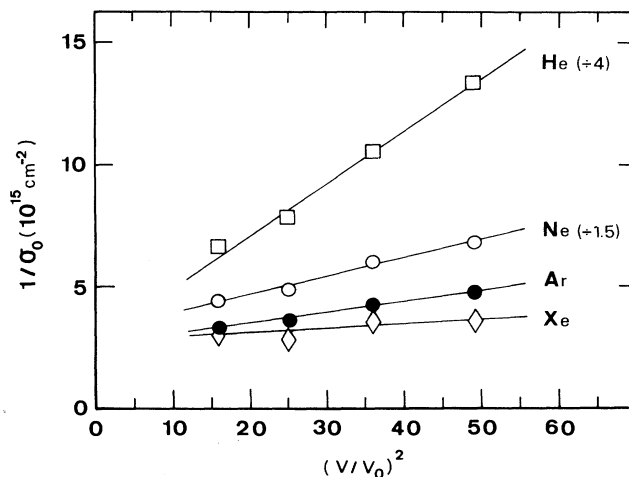

FIG. 2. Experimental neutral-production cross sections for the several targets and projectile velocities (the results are plotted as σ_0^{-1} vs v^2 and fitted to straight lines).

These facts, together with the good fits of Fig. 2, indicate that the main aspects of the phenomena are well described by this oversimplified and naive model. They also indicate that the present H production data and the H$_3^+$ destruction data of Ref. [15] show common target features.

We compared the neutral channels cross sections with that of all channels obtained from the destruction of H$_3^+$. Tables V and VI give the ratios $\sigma_0/\sigma_d^{H_3^+}$ and $\sigma_{II}/\sigma_d^{H_3^+}$ for all targets. As a general feature, we can observe that these values do not show any strong target dependence, in spite of the fact that Z varies from 2 to 54. There is a weak increase with Z for the first three targets followed in the xenon case by a decrease in values comparable to or even lower than the ones for He, this being more visible for σ_0 than for σ_{II}.

Finally, concerning only the argon target, we give in Table VII the $\sigma_{00}/\sigma_d^{H_3^+}$ and $\sigma_M/\sigma_d^{H_3^+}$ ratios. A slight increase with velocity could be noted for the former and a steeper one for the latter. Table VII data also show that σ_{00} is roughly 3 times larger than σ_M.

ACKNOWLEDGMENTS

[1] J. D. Augspurger and C. E. Dykstra, J. Chem. Phys. 88, 3817 (1988); P. E. S. Wormer and F. de Groot, *ibid.* 90, 2344 (1989); J. Tennyson, O. Brass, and E. Pollak, *ibid.* 92, 3005 (1990), and references therein.

[2] M. Farizon, B. Farizon-Mazuy, N. V. de Castro Faria, and H. Chermette, Chem. Phys. Lett. 177, 451 (1991); M. Farizon, N. V. de Castro Faria, B. Farizon-Mazuy, and M. J. Gaillard, Phys. Rev. A 45, 179 (1992), and references therein.

[3] P. Drossart, Nature (London) 340, 539 (1989), and references therein.

[4] R. K. Janev, Comments At. Mol. Phys. 26, 83 (1991), and references therein.

[5] D. L. Montgomery and D. H. Jaecks, Phys. Rev. Lett. 51, 1862 (1983); O. Yenen and D. H. Jaecks, Phys. Rev. A 32, 836 (1985); D. H. Jaecks, O. Yenen, C. Engelhardt, and L. Wiese, Nucl. Instrum. Methods, Phys. Res. Sect. B 40/41, 225 (1989); O. Yenen, D. H. Jaecks, and L. M. Wiese, Phys. Rev. A 39, 1767 (1989); O. Yenen, L. M. Wiese, D. Calabrese, and D. H. Jaecks, *ibid.* 42, 324 (1990).

[6] C. Cisneros, I. Alvarez, R. Garcia G., C. F. Barnett, J. A. Ray, and A. Russek, Phys. Rev. A 19, 631 (1979); I. Alvarez, C. Cisneros, J. de Urquijo, and T. J. Morgan, Phys. Rev. Lett. 53, 740 (1984); H. Martínez, I. Alvarez, J. de Urquijo, C. Cisneros, and A. Amaya-Tapia, Phys. Rev. A 36, 5425 (1987); I. Alvarez, H. Martínez, C. Cisneros, A. Morales, and J. de Urquijo, Nucl. Instrum. Methods, Phys. Res. Sect. B 40/41, 245 (1989); H. Martínez, I. Alvarez, C. Cisneros, and J. de Urquijo, *ibid.* 53, 267 (1991).

[7] S. C. Goh and J. B. Swan, Phys. Rev. A 24, 1624 (1981).

[8] J. B. A. Mitchell, J. L. Forand, C. T. Ng, D. P. Levac, R. E. Mitchell, P. M. Mul, W. Claeys, A. Sen, and J. Wm. McGowan, Phys. Rev. Lett. 51, 885 (1983); J. B. A. Mitchell, C. T. Ng, J. L. Forand, R. Janssen, and J. Wm. McGowan, J. Phys. B 17, L909 (1984); A. Sen and J. B. A. Mitchell, *ibid.* 19, 1545 (1986); H. Hus, F. Youssif, A. Sen, and J. B. A. Mitchell, Phys. Rev. A 38, 658 (1988); J. B. A. Mitchell, Phys. Rep. 186, 215 (1990).

[9] M. Vogler and B. Meierjohann, J. Chem. Phys. 69, 2450 (1978); M. Vogler, Phys. Rev. A 19, 1 (1979).

[10] B. Peart and K. T. Dolder, J. Phys. B 7, 1567 (1974); B. Peart, R. A. Forrest, and K. Dolder, *ibid.* 12, 3441 (1979).

[11] N. V. Fedorenko, Zh. Tekh. Fiz. 24, 769 (1954); G. W. McClure, Phys. Rev. 130, 1852 (1963); J. F. Williams and D. N. F. Dunbar, *ibid.* 149, 62 (1966); K. H. Berkner, T. J. Morgan, R. V. Pyle, and J. W. Stearns, Phys. Rev. A 8, 2870 (1973).

[12] D. Nir, B. Rosner, A. Mann, and J. Kantor, Phys. Rev. A 18, 156 (1978); S. Abraham, D. Nir, and B. Rosner, *ibid.* 29, 3122 (1984).

[13] M. J. Gaillard, A. G. de Pinho, J. C. Poizat, J. Remillieux, and R. Saoudi, Phys. Rev. A 28, 1267 (1983).

[14] N. V. de Castro Faria, M. J. Gaillard, J. C. Poizat, and J. Remillieux, Nucl. Instrum. Methods, Phys. Res. Sect. B 43, 1 (1989).

[15] W. Wolff, L. F. S. Coelho, H. E. Wolf, and N. V. de Castro Faria, Phys. Rev. A 45, 2978 (1992).

[16] N. V. de Castro Faria, W. Wolff, L. F. S. Coelho, and H. E. Wolf, Phys. Rev. A 45, 2957 (1992).

[17] Ginette Jalbert, L. F. S. Coelho, and N. V. de Castro Faria, Phys. Rev. A 46, 3840 (1992).

[18] H. Tawara, Y. Itakawa, H. Nishimura, and M. Yoshino, J. Phys. Chem. Ref. Data 19, 617 (1990).

[19] K. C. Kulander and M. F. Guest, J. Phys. B 12, L501 (1979).

[20] D. L. Smith and J. H. Futrell, J. Phys. B 8, 803 (1975); V. G. Anicich and J. H. Futrell, Int. J. Mass Spectrom. Ion Processes 55, 189 (1983/1984).

[21] D. P. Almeida, N. V. de Castro Faria, F. L. Freire, Jr., E. C. Montenegro, and A. G. de Pinho, Phys. Rev. A 36, 16 (1987).

[22] E. E. Salpeter, Proc. Phys. Soc. London, Sect. A 63, 1295 (1950).

[23] M. Meron and B. M. Johnson, Phys. Rev. A 41, 1365 (1990).

[24] D. P. Dewagan and H. R. J. Walters, J. Phys. B 11, 3983 (1978).

[25] R. Riesselman, L. W. Anderson, and L. Durand, Phys. Rev. A 43, 5934 (1991).